MODERN PATHOLOGY

USCAP
UNITED STATES AND CANADIAN ACADEMY OF PATHOLOGY
Creating a Better Pathologist

Research Article

The Complexity of Shapes: How the Circularity of Tumor Nodules Affects Prognosis in Colorectal Cancer

Nelleke P.M. Brouwer[a,*], Amjad Khan[b], John-Melle Bokhorst[a], Fazael Ayatollahi[a], Jennifer Hay[c], Francesco Ciompi[a], Femke Simmer[a], Niek Hugen[d], Johannes H.W. de Wilt[e], Martin D. Berger[f], Alessandro Lugli[b], Inti Zlobec[b], Joanne Edwards[g], Iris D. Nagtegaal[a]

[a] Department of pathology, Radboud University Medical Center, Nijmegen, The Netherlands; [b] Institute of Tissue Medicine and Pathology, University of Bern, Bern, Switzerland; [c] Glasgow Tissue Research Facility, University of Glasgow, Queen Elizabeth University Hospital, Glasgow, UK; [d] Department of surgery, Netherlands Cancer Institute, Amsterdam, The Netherlands; [e] Department of surgery, Radboud University Medical Center, Nijmegen, The Netherlands; [f] Department of Medical Oncology, Inselspital, University Hospital of Bern, University of Bern, Bern, Switzerland; [g] School of Cancer Sciences, University of Glasgow, Glasgow, UK

ARTICLE INFO

ABSTRACT

The current stratification of tumor nodules in colorectal cancer (CRC) staging is subjective and leads to high interobserver variability. In this study, the objective assessment of the shape of lymph node metastases (LNMs), extranodal extension (ENE), and tumor deposits (TDs) was correlated with outcomes. A test cohort and a validation cohort were included from 2 different institutions. The test cohort consisted of 190 cases of stage III CRC. Slides with LNMs and TDs were annotated and processed using a segmentation algorithm to determine their shape. The complexity ratio was calculated for every shape and correlated with outcomes. A cohort of 160 stage III CRC cases was used to validate findings. TDs showed significantly more complex shapes than LNMs with ENE, which were more complex than LNMs without ENE ($P < .001$). In the test cohort, patients with the highest sum of complexity ratios had significantly lower disease-free survival ($P < .01$). When only the nodule with the highest complexity was considered, this effect was even stronger ($P < .001$). This maximum complexity ratio per patient was identified as an independent prognostic factor in the multivariate analysis (hazard ratio, 2.47; $P < .05$). The trends in the validation cohort confirmed the results. More complex nodules in stage III CRC were correlated with significantly worse disease-free survival, even if only based on the most complex nodule. These results suggest that more complex nodules reflect more invasive tumor biology. As most of the more complex nodules were diagnosed as TDs, we suggest providing a more prominent role for TDs in the nodal stage and include an objective complexity measure in their definition.

Introduction

The optimal classification and treatment of patients with colorectal cancer (CRC) currently relies on staging following the tumor, node, metastasis (TNM) system. As the TNM system is based on the sequential progression hypothesis that metastases

* Corresponding author.
E-mail address: Nelleke.brouwer@radboudumc.nl (N.P.M. Brouwer).

occur as a direct consequence of lymphatic spread, lymph node metastases (LNMs) have the highest impact on the selection of patients eligible for specific treatments.[1,2] However, there is ample evidence that other histologic features such as extranodal extension (ENE) and tumor deposits (TDs) also affect prognosis.[3-5]

In the case of ENE tumors, cells extend through the nodal capsule into the perinodal fatty tissue. This has been identified as a poor prognostic factor compared with LNMs without ENE.[5,6] Additionally, TDs, referred to as isolated tumor aggregates in the fat surrounding the bowel, also have an independent prognostic impact in CRC.[3,4] Currently, ENE is not separately included in the staging of patients with CRC and TDs are categorized in the nodal stage as N1c, only having clinical impact in the absence of LNMs.[7]

An LNM can be observed as a round structure in the adipose tissue. As tumor cells break through histologic borders and form ENE, the shape of the tumor nodule becomes more irregular, demonstrating increased complexity of shape. In this perspective, the complexity of a tumor nodule might be seen as a marker for its biological behavior and thereby possibly correlates with prognosis. However, the visual estimation of histologic structures implicitly carries the subjectivity of the pathologist's opinion, as has been shown in earlier studies on TDs.[8-10] This fact undermines quantitative studies on this topic to determine the prognostic impact. The rapid developments in the field of image analysis using deep learning can overcome this subjective issue.

Owing to the novel possibilities of segmentation algorithms, that is, computer models capable of delineating the border of objects of interest automatically, it is now possible to objectively answer research questions for which a human's assessment is too subjective. In view of the possible underlying differences in biology and the prognostic impact between tumor nodules with a complex shape, this study uses computational pathology to analyze how the complexity of tumor nodules correlates with outcomes in stage III CRC.

Materials and Methods

Test Cohort

A review of a local CRC test cohort from the Institute of Tissue Medicine and Pathology (University of Bern, Switzerland) was performed. All patients diagnosed with stage III adenocarcinoma of the colon or rectum between 2002 and 2017 were included. Only cases for which all hematoxylin and eosin (H&E)-stained slides were available were included. Additionally, adenocarcinomas showing squamous, signet ring cells, or mucinous components upon histologic review were excluded, because of their different biological behavior and potential influence on the final shape of tumor nodules. All cases were reviewed for the presence of locoregional tumor nodules (ie, LNMs with or without ENE and TDs); if no tumor nodules were found, the case was excluded. This yielded a final cohort of 190 CRC cases with a total of 848 individual tumor nodules. The slides were scanned with a Panoramic P1000 digital slide scanner (3DHistech) at ×40 magnification (0.243 μm per pixel).

For all patients, disease-free survival (DFS) data were included, as well as the following clinicopathologic characteristics: (1) gender, (2) age, (3) location of the primary tumor, (4) the number of lymph nodes found on examination, (5) pathological node (pN) stage, (6) primary tumor (pT) stage, (7) the presence of vascular invasion, (8) the use of preoperative therapy, and (9) the use of postoperative therapy.

The study was approved by and in accordance with the ethical standards of the responsible committee in the canton of Bern (collected under ethics number b2021-00033).

External Validation Cohort

A cohort from the Glasgow Tissue Research Facility at the Queen Elizabeth University Hospital (University of Glasgow, UK) was used as a validation cohort for the proposed complexity ratio. Patients were selected from a local cohort of patients with CRC diagnosed between 2002 and 2013 with stage III adenocarcinoma (collected under National Health Service Greater Glasgow and Clyde Biorepository ethics 22/WS/0020). In comparison with the test cohort, the cases were reviewed and only those for which all H&E slides were available, which had adenocarcinomas without characteristics of other histologic subtypes, and for which upon review at least one tumor nodule was found, were included. The validation cohort consisted of 160 CRC cases with a total of 595 individual tumor nodules. The slides were scanned with a Hamamatsu Nanozoomer 2.0HT slide scanner (Hamamatsu) at x20 magnification (0.46 μm per pixel).

Tissue Segmentation and Shape Determination

All H&E slides were histologically reviewed and the nodules were first classified as LNMs, LNMs with ENE or TDs, following the current TNM8 guidelines and in agreement with an expert pathologist.[7] All individual nodules were manually generally annotated as regions of interest to enable the segmentation of individual nodules in case they were present on the same H&E slide. No minimum distance between tumor nodules was used. If multiple small tumor foci were present on the same slide, they were annotated as one tumor nodule when desmoplastic stroma connected the foci. If this was not the case, the foci were annotated as separate tumor nodules. Furthermore, no minimum size cutoff was used for tumor nodules.

A deep-learning model for the segmentation of colon cancer tissue was then applied. Details on the development of the deep-learning model have been described elsewhere.[11] The model was used to segment the regions of interest into the following 14 different tissue compartments: (1) normal epithelium, (2) low-grade dysplastic epithelium, (3) and (4) high-grade dysplastic/cancerous epithelium, (5) stroma lamina propria, (6) submucosal stroma, (7) desmoplastic stroma, (8) muscle, (9) nerve, (10) adipose tissue, (11) mucus, (12) and (13) necrosis and debris, and (14) background. With the exception of the background and adipose tissue, all other tissue compartments were included to identify the segmented object representing the tumor nodule. The included tissue compartments were used to create a binary mask, and small objects and holes were filled in a postprocessing step. The active contour algorithm was applied to extract the final shape of the individual nodules.[12] The workflow for annotation, segmentation, and postprocessing to come to the final shape is illustrated in Figure 1A-D.

Calculation of Complexity Ratios

To quantify the complexity of a tumor nodule's shape, the perimeter of the nodule was compared with the circumference of a perfect circle ($2\pi r$) having the same area, resulting in the following function: $\frac{nodule\ perimeter}{2\pi\sqrt{\frac{nodule\ area}{\pi}}}$. This function calculates the
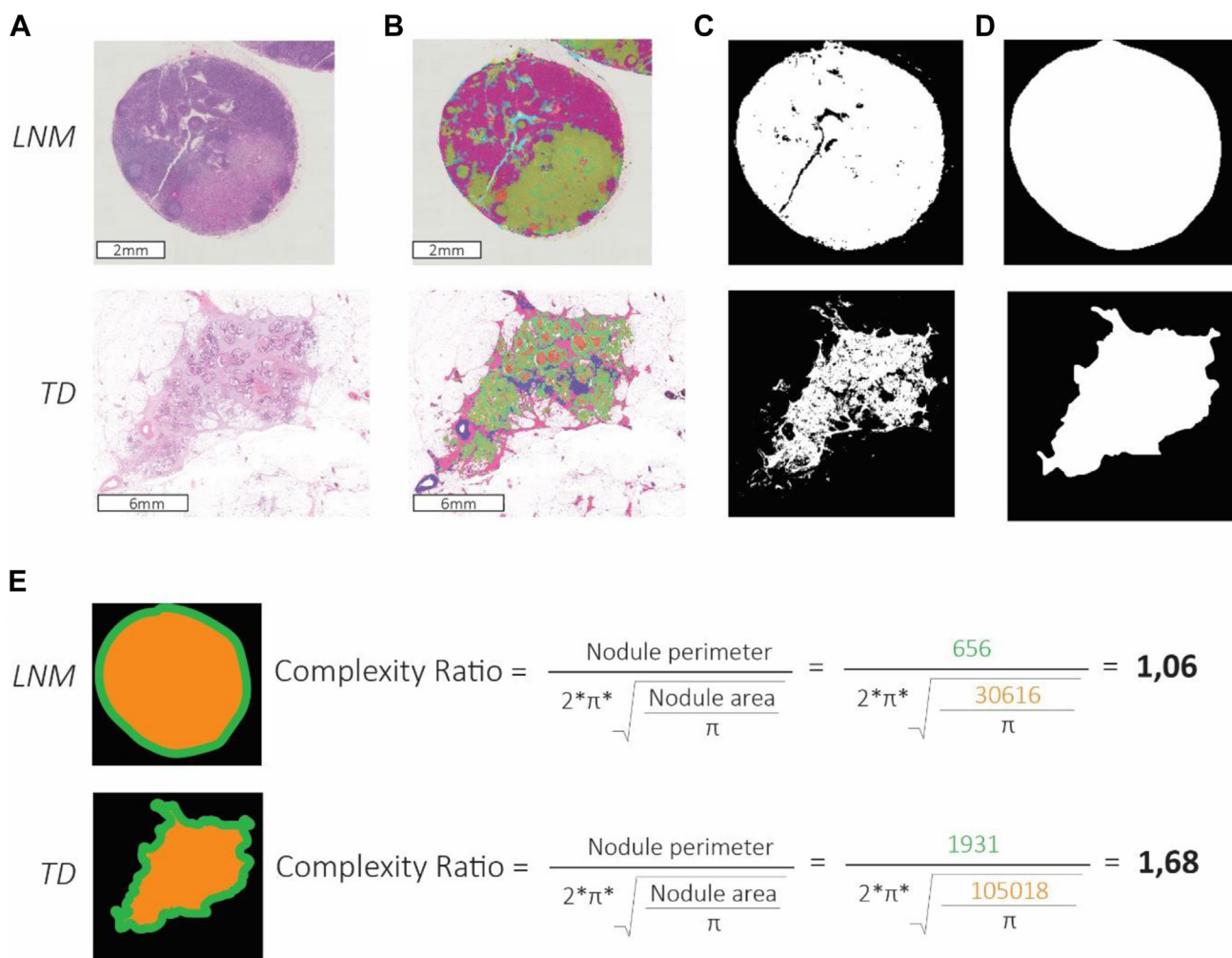
Figure 1.
The workflow of the use of the artificial intelligence algorithm to analyze the nodular shape and calculate the complexity of every nodule. (A) All hematoxylin and eosin−stained slides in which tumor nodules were found were scanned for the analysis. (B) A deep-learning model was used to segment the nodules into different tissue types. (C) Tumor cells, lymphocytes, stroma, mucus, and necrosis were included to create a binary mask. (D) The binary mask was postprocessed, and the active contour algorithm was applied to extract the final shape. (E) The complexity ratio was calculated with a ratio closer to 1.00 for round shapes and an increasing ratio for increasingly complex shapes. LNM, lymph node metastasis; TD, tumor deposit.

complexity ratio (ie, how much the roundness of the shape resembles a circle) and results in a continuous numerical value that increases as the complexity of a tumor nodule increases, starting at a complexity ratio of 1.00 for a perfectly round tumor nodule (Fig. 1E).

Statistical Analysis

The complexity ratios for different histopathologic classifications of the tumor nodules were visualized using a box plot and the statistical significance was calculated using the Kruskal-Wallis test. Survival time was defined as the time from surgical resection to disease recurrence or the end of follow-up. DFS was estimated with the Kaplan-Meier method and compared with log-rank testing. The optimal cutoff for the sum of all complexity ratios per case was determined in the test cohort using maximally selected rank statistics. This approach uses a computer algorithm that facilitates categorization of observations into 2 groups on the basis of the maximum significance by a continuous or ordinal variable.[13] However, this measure of complexity is potentially biased by the number of involved nodes. Therefore, a second measure of complexity was determined: the maximum of complexity. For this measure, only the most complex nodule per case was included and the total number of tumor nodules was disregarded. Again, the optimal cutoff was determined for the test cohort using maximally selected rank statistics. Clinicopathologic characteristics were assessed according to the maximum complexity ratio using the Pearson's χ^2 test for categorical variables and the Wilcoxon rank sum test for continuous variables. Univariate and multivariate Cox regression analyses were performed to identify the clinicopathologic variables associated with DFS in both the test and the external validation cohort to analyze if the results of the test cohort were generalizable. All covariates that were significant in the univariate analysis were included in the multivariate model. Using the multivariate models for the test and validation cohorts, a survival area plot was generated. Instead of plotting value-specific curves, the probability of DFS was represented as an area in which the color changes according to the continuous variable (ie, the maximum complexity ratio). The

relative importance of all covariates was analyzed to quantify the relative weight of individual factors in determining the DFS. A *P* value of <.05 was considered statistically significant for all analyses. Hazard ratios (HRs) and risk ratios were presented with a 95% CI. RStudio (PBC) (RStudio Team [2020]. RStudio: Integrated Development for R. URL: http://www.rstudio.com/) was used for all analyses.

Results

In total, 190 patients were included in the test cohort and 160 in the validation cohort. As expected, both the test and the validation cohort showed higher survival rates for pN1 compared with pN2 with a significance value of *P* < .01 (Supplementary Fig. S1).

Complexity of Different Types of Tumor Nodules

In the test cohort, a total of 848 nodules (1-35 nodules per case) were segmented and their shapes analyzed for complexity. Figure 2 shows that LNMs have a round shape with a complexity ratio closer to 1.0. LNMs with ENE had a significantly more complex shape (*P* < .001) when compared with LNMs without ENE. In general, TDs were the most complex compared with LNMs with ENE (*P* < .01) and LNMs without ENE (*P* < .001). The validation cohort showed similar results (Supplementary Fig. S2). The size of tumor nodules did not correlate with their complexity ratio (Supplementary Fig. S3).

Correlation Between Complexity and Clinicopathologic Characteristics

The majority of clinicopathologic characteristics showed no significant differences between low and high maximum

Figure 2.
A box plot showing the complexity ratio of 3 different histologically defined nodule types in the test cohort; TDs, ENE, and LNMs. Statistical significance was calculated using the Kruskal-Wallis test. **P < .01; ***P < .001. ENE, extranodal extension; LNM, lymph node metastase; TD, tumor deposit.

complexity, both in the test and the validation cohort (Table 1). The only pathological characteristic that differed was the pN stage with more pN2 in the high maximum complexity group (51% vs 13% in the low maximum complexity group; *P* < .01). However, it is important to note that the maximum complexity ratio is not a surrogate for the pN stage as 49% and 57% of cases in the high complexity group were pN1 in the test and the validation cohort, respectively.

Complexity of Tumor Nodules Affects Prognosis

For the majority of patients in both cohorts, multiple tumor nodules were found, all with their own complexity ratios. When the complexity ratios of all tumor nodules were summed up with a cutoff of 4.00, the DFS was significantly higher for patients with a low sum of complexity (*P* = .003; Fig. 3A). Using the maximum complexity ratio with a cutoff of 1.47, the cases with a low maximum complexity ratio still showed significantly higher DFS than those with a high maximum complexity ratio (*P* < .001; Fig. 3B).

Patients with a high maximum complexity ratio had an increased risk for disease recurrence (risk ratio = 3.10; 95% CI, 1.49-6.48) compared with patients with a low maximum complexity ratio. In the univariate cox regression analysis, left-sided tumor location, pN2 stage, and the maximum complexity ratio were significantly associated with DFS (Table 2). In the multivariate analysis, the HR for the maximum complexity ratio remained significant (2.47; 95% CI, 1.04-5.87). Analysis of the relative importance of all covariates revealed that the maximum complexity ratio was the most important variable (30%), then the total number of lymph nodes found (21%) and vascular invasion (12%; Supplementary Fig. S4A). When only the covariates included in the final multivariate model were analyzed, the maximum complexity ratio was the most important variable (39%; Supplementary Fig. S4B).

External Validation

The external validation cohort consisted of 160 patients with 1 to 23 nodules per case and comprised relatively younger patients (a mean age of 67.7 years compared with 70.9 in the test cohort; *P* = .01) and a larger proportion of cases with vascular invasion (74% compared with 60% in the test cohort; *P* < .01). It also showed a smaller proportion of patients who underwent postoperative therapy (48% compared with 68% in the test cohort; *P* < .01) and a lower mean number of lymph nodes found upon pathological examination (17.8 compared with 26.1 in the test cohort; *P* < .01). The rest of the clinicopathologic parameters were not significantly different between the test and the validation cohort (Table 1).

The complexity ratios showed a similar distribution for the different types of tumor nodules in the validation cohort when compared with the test cohort, although generally the tumor nodules were less complex (Supplementary Fig. S5). The maximum complexity ratio determined in the test cohort (1.47) was also applied as a cutoff in the validation cohort and again showed a significant correlation with DFS (Supplementary Fig. S6 and Table 3) with an HR in the univariate cox regression analysis of 1.7 (95% CI, 1.01-2.87). When pN stage, pT stage, vascular invasion, differentiation grade, and the maximum complexity ratio were included in the multivariate Cox
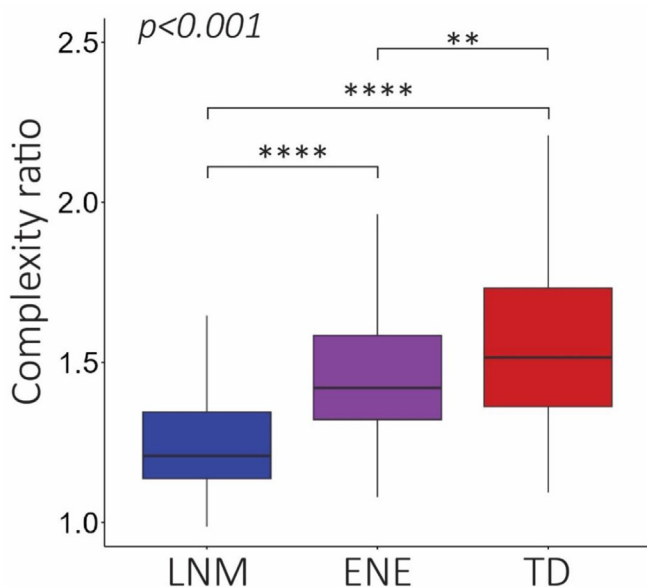
Table 1

Clinicopathologic characteristics of patients in the test and the validation cohort, according to low or high complexity of the most complex nodule

| Covariate | Test cohort (n = 190) | | | | | | | Validation cohort (n = 169) | | | | | | | Test vs validation |
| | Low complexity n = 91 (48%) | | High complexity n = 99 (52%) | | Total | | | Low complexity n = 113 (72%) | | High complexity n = 47 (28%) | | Total | | | |
	n	(%)	n	(%)	n	(%)	P	n	(%)	n	(%)	n	(%)	P	P
Gender															
Male	52	(57)	65	(66)	117	(62)	.23	60	(53)	26	(55)	86	(54)	.80	.17
Female	39	(43)	34	(34)	73	(38)		53	(47)	21	(47)	74	(46)		
Age (y)															
Mean (SD)	72.2 (12.8)		69.8 (12.9)		70.9 (12.9)		.16	67.3 (11.1)		68.7 (10.3)		67.7 (10.9)		.46	.01
Tumor location															
Right	32	(36)	22	(23)	54	(29)	.10	47	(42)	16	(34)	63	(39)	.65	.06
Left	36	(40)	42	(43)	78	(42)		38	(34)	17	(36)	55	(34)		
Rectum	21	(24)	33	(34)	54	(29)		28	(25)	14	(30)	42	(26)		
Unknown	2		2		4										
No. of lymph nodes found															
Mean (SD)	25.5 (11.1)		26.7 (14.2)		26.1 (12.7)		.71	17.8 (7.6)		17.9 (6.1)		17.8 (7.2)		.57	<.01
pN stage															
1	79	(87)	49	(49)	128	(67)	<.01	87	(77)	27	(57)	114	(71)	.01	.50
2	12	(13)	50	(51)	62	(33)		26	(23)	20	(43)	46	(29)		
pT stage															
1	3	(3)	1	(1)	4	(2)	.46	1	(1)	0	(0)	1	(1)	.06	.21
2	8	(9)	10	(10)	18	(9)		7	(6)	0	(0)	7	(4)		
3	56	(62)	54	(55)	110	(58)		61	(54)	20	(43)	81	(51)		
4	24	(26)	34	(35)	58	(30)		44	(39)	27	(57)	71	(44)		
Differentiation grade															
Well	1	(2)	0	(0)	1	(1)	.73	2	(2)	0	(0)	2	(1)	.89	.17
Moderate	72	(86)	76	(88)	148	(87)		98	(87)	43	(91)	141	(88)		
Poor	11	(13)	10	(12)	21	(12)		13	(12)	4	(9)	17	(11)		
Unknown	7		13		20										
Vascular invasion															
Yes	50	(57)	59	(63)	109	(60)	.36	80	(71)	39	(83)	119	(74)	.11	<.01
No	38	(43)	34	(37)	72	(40)		33	(29)	8	(17)	41	(26)		
Unknown	5		4		9										
MMR status															
dMMR (MSI)	11	(12)	8	(8)	19	(10)	.39	14	(13)	10	(23)	24	(16)	.10	<.01
pMMR (MSS)	79	(88)	87	(92)	166	(90)		97	(87)	33	(77)	130	(84)		
Unknown	1		4		5			2		4		6			
Preoperative therapy															
Yes	11	(12)	22	(22)	33	(17)	.07								<.01
No	80	(88)	77	(78)	157	(83)		113	(100)	47	(100)	160	(100)	NA	
Postoperative therapy															
Yes	39	(60)	52	(76)	91	(68)	.04	54	(48)	23	(49)	77	(48)	.89	<.01
No	26	(40)	16	(24)	42	(32)		59	(52)	24	(51)	83	(52)		
Unknown	26		31		57										

The P value corresponds to the Pearson's χ^2 test for qualitative measurements and to the analysis of variance test for quantitative measures. The difference in each cohort is calculated in relation to its distribution between low and high maximum complexity, as well as an overall comparison between the 2 cohorts.

dMMR, deficient mismatch repair; MMR, mismatch repair; MSI, microsatellite instable; MSS, microsatellite stable; NA, not applicable; pMMR, proficient mismatch repair; pN, pathological node; pT, primary tumor.
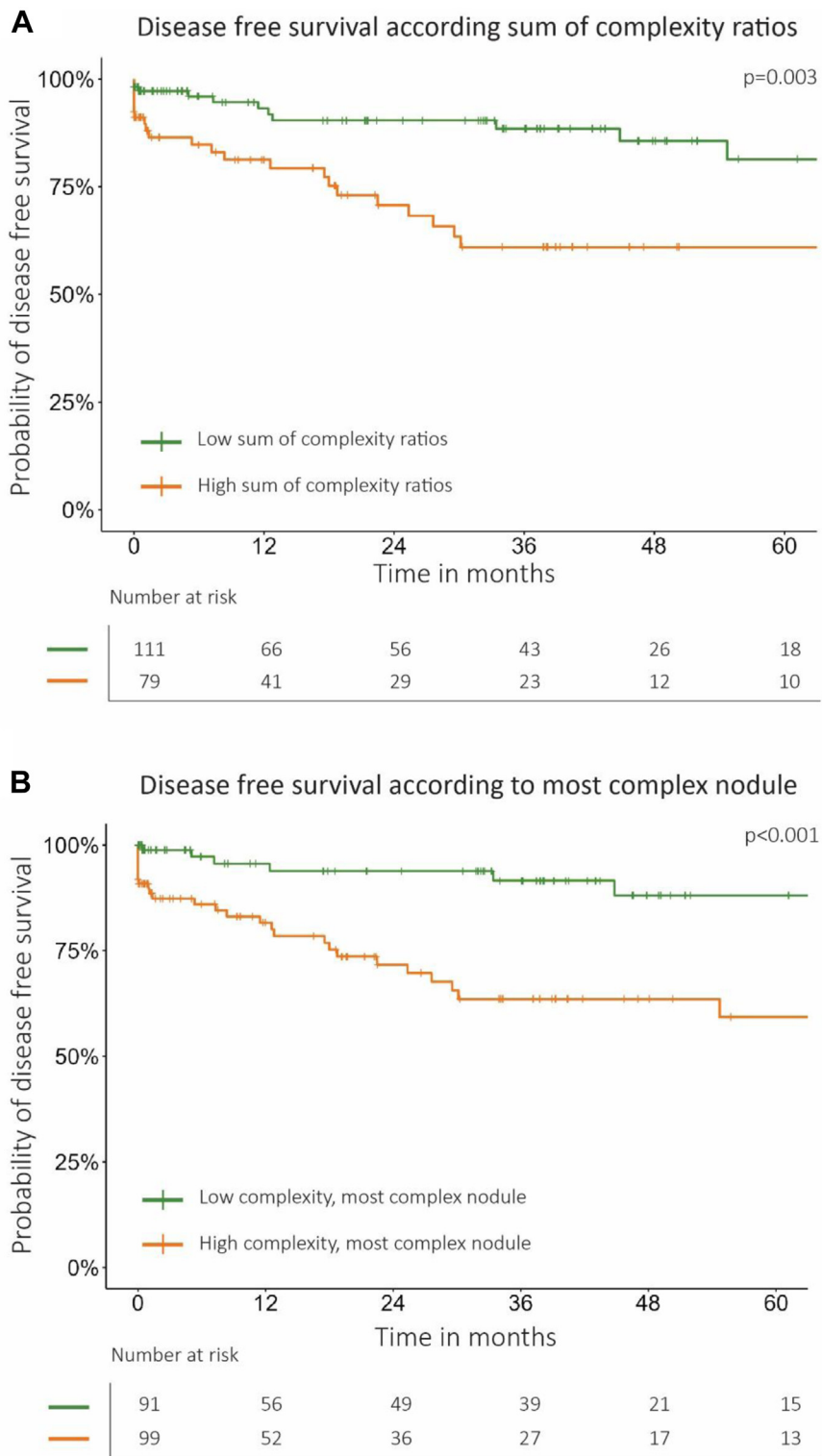
Figure 3.
Kaplan-Meier curves showing the impact of complexity ratios on disease-free survival in the test cohort. (A) Disease-free survival analysis according to the sum of all complexity ratios per patient. (B) Disease-free survival analysis solely according to the most complex nodule per patient.

regression analysis, the maximum complexity ratio was no longer significant.

As additional subanalyses, the Kaplan-Meier curves for TD-positive cases has been added for the combined cohorts (Supplementary Fig. S7). As expected, prognosis deteriorated from N1 (including N1c) to N2. There was still a clear difference in prognosis based on complexity, but owing to the limited numbers, this approached significance in this subgroup (*P* = .054).

Table 2
Univariate and multivariate analyses of factors associated with disease-free survival in the test cohort

Covariate	Number	(%)	Univariate analysis			Multivariate analysis		
			HR	95% CI	P	HR	95% CI	P
Gender								
Male	117	(62)	1.17	(0.58-2.35)	.66			
Female	73	(38)	(1.00)					
Age (y)								
Mean (SD)	70.9	(12.9)	1.00	(0.97-1.03)	.87			
Tumor location								
Right	54	(29)	(1.00)			(1.00)		
Left	78	(42)	3.32	(1.23-8.97)	.02	2.71	(1.00-7.37)	.05
Rectum	54	(29)	2.50	(0.83-7.49)	.1	1.97	(0.65-5.95)	.22
No. of lymph nodes found								
Mean (SD)	26.1	(12.7)	1.03	(0.94-1.01)	.1			
pN stage								
1	128	(67)	(1.00)			(1.00)		
2	62	(33)	2.67	(1.37-5.19)	<.01	1.81	(0.87-3.79)	.11
pT stage								
1	4	(2)	0.77	(0.00-∞)	.997			
2	18	(9)	0.39	(0.09-1.72)	.214			
3	110	(58)	0.00	(0.38-1.55)	.468			
4	58	(30)	(1.00)					
Differentiation grade								
Well	1	(1)	0.00	(0.00-∞)	1.00			
Moderate	148	(87)	1.00	(0.35-2.86)	1.00			
Poor	21	(12)	(1.00)					
Vascular invasion								
Yes	109	(60)	0.88	(0.44-1.75)	.71			
No	72	(40)	(1.00)					
MMR status								
dMMR (MSI)	19	(10)	0.54	(0.13-2.28)	.40			
pMMR (MSS)	166	(90)	(1.00)					
Preoperative therapy								
Yes	33	(17)	0.99	(0.98-1.01)	.22			
No	157	(83)	(1.00)					
Postoperative therapy								
Yes	91	(68)	1.33	(0.56-3.13)	.52			
No	42	(32)	(1.00)					
Most complex nodule								
Not complex	91	(48)	(1.00)			1.00		
Complex	99	(52)	3.56	(1.61-7.85)	<.01	2.47	(1.04-5.87)	<.05

For each covariate, the individual hazard ratio is calculated with a Cox proportional hazard model. All covariates with a statistically significant individual hazard ratio were included in the multivariate analysis.
dMMR, deficient mismatch repair; HR, hazard ratio; MMR, mismatch repair; MSI, microsatellite instable; MSS, microsatellite stable; pMMR, proficient mismatch repair; pN, pathological node; pT, primary tumor.

Preoperative Treatment Does Not Influence the Prognostic Impact of Complexity

Tumor nodules from preoperatively treated cases had a lower median complexity ratio (*P* = .01; Supplementary Fig. S8). When the test cohort was stratified according to receiving preoperative treatment in a subanalysis, the worse prognosis for cases with a high maximum complexity ratio remained. This was significant in the nonpreoperatively treated group (*P* = .001) but not in the preoperatively treated group, due to a low number of cases (n = 33; Supplementary Fig. S9). As the validation cohort consisted only of nonpreoperatively treated cases, these subanalyses were only performed for the test cohort.

The Prognostic Impact of Complexity Is a Continuum

To optimize the analytical power, the maximum complexity ratio was used as a categorical variable in the univariate and multivariate analysis, labeling cases as either of high or of low complexity. Still, when the survival area is plotted for DFS according to the maximum complexity ratio, it can be appreciated that the prognostic impact of the complexity ratio is a continuum. A low maximum complexity ratio is related to better survival, which gradually decreases as the maximum complexity increases (Fig. 4).

Discussion

This study shows that the shape of tumor nodules is associated with prognosis in stage III CRC. By objectively measuring the shape of tumor nodules using the complexity ratio, it was found that patients with more complex tumor nodules have worse 5-year DFS. This correlation was even more pronounced when only the most complex nodule of every case was taken into account. The trends in the external validation cohort confirmed these findings.

Table 3
Univariate and multivariate analyses of factors associated with disease-free survival in the validation cohort

Covariate	Number	(%)	Univariate analysis			Multivariate analysis		
			HR	95% CI	P	HR	95% CI	P
Gender								
Male	86	(54)	1.30	(0.78-2.17)	.32			
Female	74	(46)	(1.00)					
Age (y)								
Mean (SD)	67.7	(10.9)	1.00	(0.98-1.03)	1.00			
Tumor location								
Right	63	(39)	(1.00)					
Left	55	(34)	0.93	(0.52-1.67)	.81			
Rectum	42	(26)	0.96	(0.51-1.81)	.91			
No. of lymph nodes found								
Mean (SD)	17.8	(7.2)	0.98	(0.94-1.02)	.28			
pN stage								
1	114	(71)	(1.00)			(1.00)		
2	46	(29)	2.05	(1.23-3.43)	<.01	1.88	(1.11-3.18)	<.05
pT stage								
1	1	(1)	0.00	(0.00-∞)	1	0.00	(0.00-∞)	1
2	7	(4)	0.65	(0.20-2.12)	.48	1.49	(0.41-5.49)	.55
3	81	(51)	0.46	(0.27-0.77)	<.01	0.57	(0.33-0.98)	<.05
4	71	(44)	(1.00)			(1.00)		
Differentiation grade								
Well	2	1	0.00	(0.00-∞)	1	0.00	(0.00-∞)	1
Moderate	141	88	0.40	(0.20-0.79)	<.01	0.43	(0.21-0.87)	<.05
Poor	17	11	1.00			(1.00)		
Vascular invasion								
Yes	119	(74)	1.94	(1.01-3.73)	<.05	2.01	(1.00-4.06)	.05
No	41	(26)	(1.00)			(1.00)		
MMR status								
dMMR (MSI)	24	(16)	0.49	(0.87-3.08)	.13			
pMMR (MSS)	130	(84)	(1.00)					
Postoperative therapy								
Yes	91	(68%)	1.33	(0.56-3.13)	.52			
No	42	(32%)	(1.00)					
Most complex nodule								
Not complex	91	(48%)	(1.00)			(1.00)		
Complex	99	(52%)	3.56	(1.61-7.85)	<.01	1.50	(0.87-2.59)	.18

For each covariate, the individual hazard ratio is calculated with a Cox proportional hazard model. All covariates with a statistically significant individual hazard ratio were included in the multivariate analysis.
dMMR, deficient mismatch repair; HR, hazard ratio; MMR, mismatch repair; MSI, microsatellite instable; MSS, microsatellite stable; pMMR, proficient mismatch repair; pN, pathological node; pT, primary tumor.

Using a segmentation algorithm to analyze 1443 individual tumor nodules, this study was the first to overcome the subjectiveness of human assessment of shape in CRC. Our study shows that the complexity of tumor nodules increased from LNMs without ENE, to LNMs with ENE, to TDs. As increased complexity was associated with worse prognosis, our results are in line with studies using histopathologic definitions in which the prognosis of both LNMs with ENE and TDs is worse than that of LNMs without ENE.[3,6,14] The finding that tumor nodules with a more complex shape are associated with worse DFS compared with those with a less complex shape is in contrast with a previous study in which it was found that the contour of TDs was not associated with prognosis.[15] However, there are several differences between both studies that should be emphasized. The study by Ueno et al[15] was a single-center study with a smaller sample size and a pathologist's assessment was used, whereas the current study used a segmentation algorithm. Furthermore, Ueno et al[15] only investigated TDs and did not include LNMs or ENE, but did include vascular invasion as a specific type of TD. As vascular invasion (ie, foci confined to a vascular space) is mostly observed as a round or smooth structure, it is very well possible that TDs with a smooth contour are mainly cases of vascular invasion. Vascular invasion was not included in the analyses in our study as it is not part of the nodal category in the TNM8 staging system.[7] Finally, Ueno et al[15] used overall survival as an outcome measure while we analyzed DFS. These differences make it difficult to compare findings from both studies.

The final shape of the tumor nodules analyzed in the current study consisted of several different tissue segments, with tumor cells and the reactive stroma being important determinants of the final shape. The biological explanation for the association between the complexity of shape and prognosis is most likely to be found in these 2 segments. For the tumor segment, it is known that a more irregular border, with more small clusters of tumor cells or single tumor cells (ie, tumor budding), is associated with worse prognosis. The tumor cells involved in budding undergo epithelial to mesenchymal transition (EMT), making them more invasive and more likely to metastasize.[16] The research on tumor budding focuses on the invasive front of the primary tumor, but these biological characteristics are likely to be present in complex tumor nodules as well. Regarding the stroma segment, it has been widely established that cancer invasion and the risk of metastatic spread
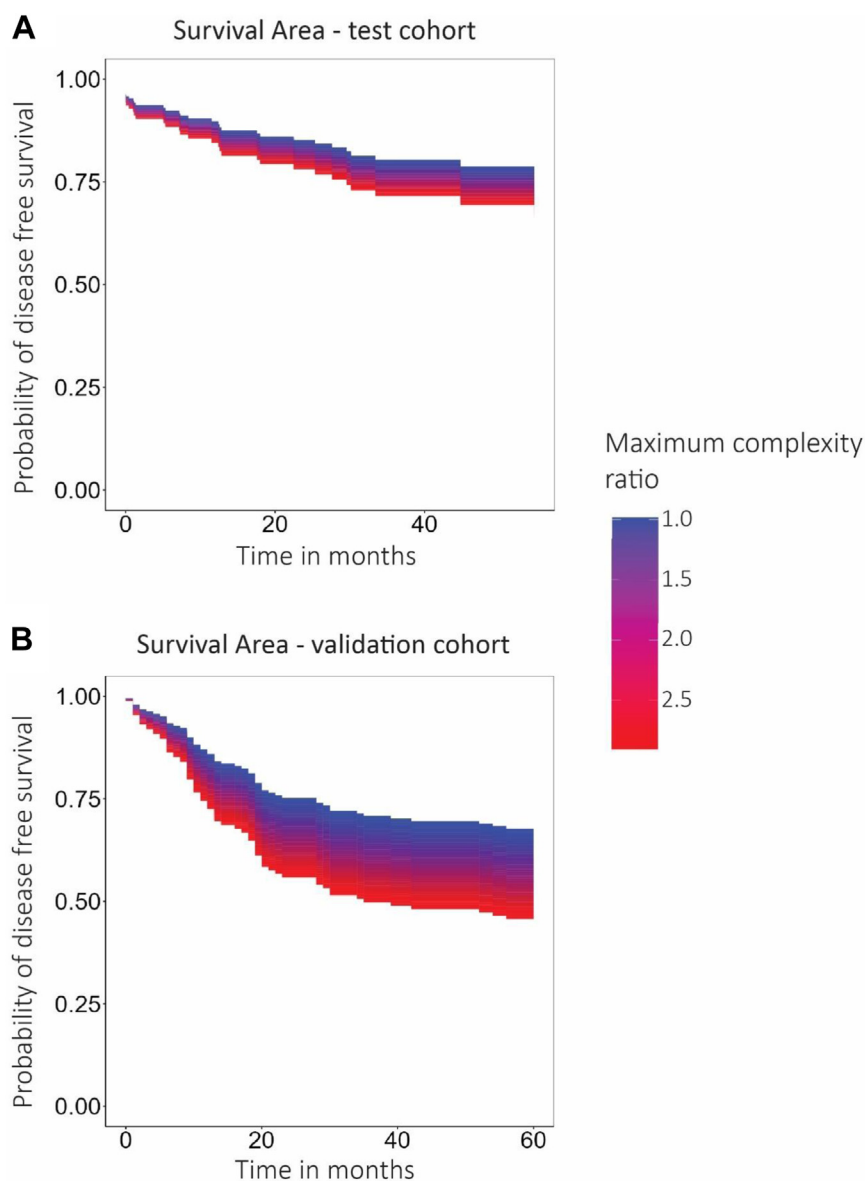
Figure 4.
The survival area plot according to the maximum complexity ratio. The survival probability curves were obtained from a multivariate cox proportional hazard model. (A) The survival area for the test cohort. Variables included in the cox proportional hazard model were tumor location, pN stage, and the maximum complexity ratio. (B) The survival area for the validation cohort. Variables included in the cox proportional hazard model were pN stage, pT stage, differentiation grade, vascular invasion, and the maximum complexity ratio.

is an interplay between the tumor cells and their microenvironment.[17] The tumor stroma has been identified as an important determinant of progression of CRC, as it can facilitate the survival and proliferation of tumor cells and promote EMT.[18-20] Indeed, a higher proportion of tumor stroma has been associated with poorer survival in CRC.[21] The combination of both a more irregular shape of the tumor segment and more tumor stroma suggests a more invasive biological phenotype for more complex tumor nodules that could influence prognosis.

Most of the more complex nodules were histologically defined as TDs. We have previously shown that TDs have a more invasive phenotype than LNMs, both in the tumor cells and in the tumor microenvironment.[22] The continuous association between the complexity of tumor nodules and prognosis (Fig. 4) could reflect the transition from an LNM (low complexity) to a TD (high complexity). This process starts with tumor cells in LNMs, acquiring the capability of crossing the lymphatic capsule and developing ENE, which slowly increases the complexity as well as the aggressive biology of the tumor nodule. Tumor cells that are able to migrate through the extracellular matrix and across histologic borders demonstrate important characteristics that are needed for further metastasis.[23] The fact that single tumor cells in LNMs (ie, micrometastases) have less prognostic impact than macrometastases in LNMs, which are again less detrimental than ENE, supports this hypothesis.[14,24] When the process continues and tumor cells further invade the adipose tissue, destroy the remnants of the lymph node, and cause the development of the tumor stroma, the shape gradually becomes more complex. Then, when the lymph node structure is no longer recognizable, the tumor nodule is defined as a TD that has a phenotype that is

characterized by EMT, invasion, and matrix remodeling.[22] Therefore, it has been suggested that the ability to break through histologic boundaries is the most important prognostic characteristic of ENE and TDs.[25,26] Still, further research is needed to see if the invasive biology of complex nodules is reflected in a direct relation with distant metastases.

The TNM8 definition asks pathologists to stratify TDs on the basis of their origin, by identifying histologic structures such as vessels, nerves, and lymphatic tissue.[7] In line with our biological explanation for the development of complex nodules, it has been shown that the shape of TDs is not associated with their possible origin.[25] Therefore, it might be less important to identify the form of locoregional spread (LNM, venous invasion, or perineural invasion) from which a complex nodule arises. Conversely, emphasis should be put on the fact that the tumor nodule has acquired more aggressive characteristics, which could increase the risk of further cancer spread. This could imply that the definition of TDs used in the TNM8 guidelines could be overly complicated. Furthermore, as most tumor nodules with high complexity ratios were histologically defined as TDs, the complexity of shapes could be added to refine the definition for TDs and LNMs in the TNM system. This is currently the case in radiology in which the distinction between LNMs and TDs is only made based on the subjective assessment of shape complexity.[27,28] With the higher impact on prognosis of more complex nodules, which is in line with previous studies showing that TDs have more prognostic impact than LNMs, TDs should be given a more prominent role in staging.[4]

The present study also has limitations. First, retrospective data analyses may have resulted in selection bias. Second, the maximum complexity ratio was no longer a significant prognostic factor in the multivariate analysis for the validation cohort. This can be explained by the effects of interinstitute variation on the segmentation algorithm. The H&E staining in the external validation cohort was less dark with paler shades than the segmentation algorithm was trained for, yielding a leftward shift of all complexity ratios (Supplementary Fig. S5). This made the cutoff for maximum complexity suboptimal for this cohort. The issues that come with interinstitute variation regarding the quality of stains are wellknown in histopathologic artificial intelligence (AI),[29] and these can only be resolved by further innovations in this field such as color-optimizing algorithms. For the severe discoloration in our validation cohort, no suitable solution was available. However, when the cutoff was adjusted for this discoloration and shifted leftward to a value of 1.38, the maximum complexity remained significant in the multivariate analysis in the validation cohort. This strengthens the findings of the study but highlights the caution that should be taken when using segmentation algorithms in external cohorts.

This study is an example of how to use AI and segmentation algorithms more specifically to overcome the limitations caused by the subjective assessment by the human eye. With the successful and rapid increase in different AI tools in pathology, many additional ways of answering research questions can be explored.[30] In clinical practice, the presence of computer-aided diagnosis systems applied to digital pathology images could assist pathologists in their assessment of tumor nodules.[31]

The results from this study can be interpreted for use in a scenario without AI in daily practice, and in one in which AI is widely implemented in the diagnostic workflow. Currently, AI is of limited use in daily practice. However, this study shows that the complexity of nodules has a prognostic impact. Even though the visual assessment of a pathologist is subjective, complexity can still be taken into account when in doubt on how to classify a tumor nodule. As most of the more complex nodules were diagnosed as TDs, irrespective of their origin, we suggest providing a more prominent role for TDs in the nodal stage and possibly include an objective complexity measure in their definition. Furthermore, in the scenario in which AI is widely implemented in the diagnostic workflow of pathologists, a segmentation algorithm can assist pathologists in determining the final shape of a nodule as well as immediately generating a complexity score with it to aid them in deciding how to define this nodule.

In conclusion, we have demonstrated that more complex tumor nodules in stage III CRC were associated with significantly worse DFS. The association between the complexity of tumor nodules and prognosis was of a continuous nature, which could be a reflection of dynamic biological processes that are reflected in the final shape. As most of the more complex nodules were diagnosed as TDs, irrespective of their origin, we suggest providing a more prominent role for TDs in the nodal stage and possibly include an objective complexity measure in their definition.

Author Contributions

This study was conceptualized and performed by N.P.M.B., J.-M.B., and I.D.N. in the Radboudumc (Nijmegen, NL), using cohorts from collaborating partners. The test cohort was provided by the Institute of Tissue Medicine and Pathology (Bern, CH) in collaboration with A.K., M.D.B., I.Z., and A.L. The validation cohort was provided by the Glasgow Tissue Research Facility at Queen Elizabeth University Hospital (Glasgow, UK) in collaboration with J.H.W.W. and J.E. N.P.M.B. and I.D.N. performed study concept and design. N.P.M.B., I.D.N., F.S., and N.H. performed the development of methodology and writing, and review and revision of the paper. N.P.M.B., A.K., J.-M.B, and F.A. provided acquisition, analysis, and interpretation of data, and statistical analysis. J.H.W.W., M.D.B., I.Z., and J.E. provided technical and material support. All authors read and approved the final paper.

Data Availability

The raw clinical data discussed in this study are not publicly available due to patient privacy guidelines but are available from the corresponding author upon reasonable request. Other data generated in this study are available within the article and supporting information data files.

Funding

The authors received no specific funding for this work.

Declaration of Competing Interest

F.C. was Chair of the Scientific and Medical Advisory Board of TRIBVN Healthcare, France, and has been receiving advisory board fees from TRIBVN Healthcare, France, for the last 5 years. He is a shareholder of Aiosyn BV, the Netherlands. M.D.B. is Medical Advisor at Aiosyn BV.

The other authors declare no conflicts of interest.

References

1. Dukes CE. The classification of cancer of the rectum. *J Pathol Bacteriol*. 1932;35(3):323—332.
2. Shinto E, Ike H, Hida JI, et al. Proposal of a modified subclassification system for stage III colorectal cancer: a multi-institutional retrospective analysis. *Ann Gastroenterol Surg*. 2020;4(6):667—675.
3. Lord AC, D'Souza N, Pucher PH, et al. Significance of extranodal tumour deposits in colorectal cancer: a systematic review and meta-analysis. *Eur J Cancer*. 2017;82:92—102.
4. Nagtegaal ID, Knijn N, Hugen N, et al. Tumor deposits in colorectal cancer: improving the value of modern staging-a systematic review and meta-analysis. *J Clin Oncol*. 2017;35(10):1119—1127.
5. Veronese N, Nottegar A, Pea A, et al. Prognostic impact and implications of extracapsular lymph node involvement in colorectal cancer: a systematic review with meta-analysis. *Ann Oncol*. 2016;27(1):42—48.
6. Ambe PC, Gödde D, Störkel S, Zirngibl H, Bönicke L. Extra nodular metastasis is a poor prognostic factor for overall survival in node-positive patients with colorectal cancer. *Int J Colorectal Dis*. 2018;33(4):403—409.
7. Brierley JD, Gospodarowicz MK, Wittekind CH, eds. *International Union Against Cancer TNM Classification of Malignant Tumours*. 8th ed. Wiley-Blackwell; 2017.
8. Howarth SM, Morgan JM, Williams GT. The new (6th edition) TNM classification of colorectal cancer–a stage too far. *Gut*. 2004;53:A21+.
9. Nagtegaal ID, Tot T, Jayne DG, et al. Lymph nodes, tumor deposits, and TNM: are we getting better? *J Clin Oncol*. 2011;29(18):2487—2492.
10. Brouwer NPM, Lord AC, Terlizzo M, et al. Interobserver variation in the classification of tumor deposits in rectal cancer-is the use of histopathological characteristics the way to go? *Virchows Arch*. 2021;479(6):1111—1118.
11. Bokhorst JM, Nagtegaal ID, Fraggetta F, et al. Deep learning for multi-class semantic segmentation enables colorectal cancer detection and classification in digital pathology images. *Sci Rep*. 2023;13(1):8398.
12. Márquez-Neila P, Baumela L, Alvarez L. A morphological approach to curvature-based evolution of curves and surfaces. *IEEE Trans Pattern Anal Mach Intell*. 2014;36(1):2—17.
13. Hothorn T, Lausen B. On the exact distribution of maximally selected rank statistics. *Comput Stat Data An*. 2003;43(2):121—137.
14. Kim CW, Kim J, Yeom SS, et al. Extranodal extension status is a powerful prognostic factor in stage III colorectal cancer. *Oncotarget*. 2017;8(37):61393—61403.
15. Ueno H, Mochizuki H, Hashiguchi Y, et al. Extramural cancer deposits without nodal structure in colorectal cancer: optimal categorization for prognostic staging. *Am J Clin Pathol*. 2007;127(2):287—294.
16. De Smedt L, Palmans S, Andel D, et al. Expression profiling of budding cells in colorectal cancer reveals an EMT-like phenotype and molecular subtype switching. *Br J Cancer*. 2017;116(1):58—65.
17. Tauriello DV, Calon A, Lonardo E, Batlle E. Determinants of metastatic competency in colorectal cancer. *Mol Oncol*. 2017;11(1):97—119.
18. Hewitt RE, Powe DG, Carter GI, Turner DR. Desmoplasia and its relevance to colorectal tumour invasion. *Int J Cancer*. 1993;53(1):62—69.
19. Sandberg TP, Stuart M, Oosting J, Tollenaar R, Sier CFM, Mesker WE. Increased expression of cancer-associated fibroblast markers at the invasive front and its association with tumor-stroma ratio in colorectal cancer. *BMC Cancer*. 2019;19(1):284.
20. Park JH, Richards CH, McMillan DC, Horgan PG, Roxburgh CSD. The relationship between tumour stroma percentage, the tumour microenvironment and survival in patients with primary operable colorectal cancer. *Ann Oncol*. 2014;25(3):644—651.
21. Sullivan L, Pacheco RR, Kmeid M, Chen A, Lee H. Tumor stroma ratio and its significance in locally advanced colorectal cancer. *Curr Oncol*. 2022;29(5):3232—3241.
22. Brouwer NPM, Webbink L, Haddad TS, et al. Transcriptomics and proteomics reveal distinct biology for lymph node metastases and tumour deposits in colorectal cancer. *J Pathol*. Published online October 4, 2023. https://doi.org/10.1002/path.6196
23. Cao H, Xu E, Liu H, Wan L, Lai M. Epithelial-mesenchymal transition in colorectal cancer metastasis: a system review. *Pathol Res Pract*. 2015;211(8):557—569.
24. Sloothaak DA, Sahami S, van der Zaag-Loonen HJ, et al. The prognostic value of micrometastases and isolated tumour cells in histologically negative lymph node of patients with colorectal cancer: a systematic review and meta-analysis. *Eur J Surg Oncol*. 2014;40(3):263—269.
25. Wünsch K, Müller J, Jähnig H, Herrmann RA, Arnholdt HM, Märkl B. Shape is not associated with the origin of pericolonic tumor deposits. *Am J Clin Pathol*. 2010;133(3):388—394.
26. Brouwer NPM, Nagtegaal ID. Tumor deposits improve staging in colon cancer: what are the next steps? *Ann Oncol*. 2021;32(10):1209—1211.
27. D'Souza N, Shaw A, Lord A, et al. Assessment of a staging system for sigmoid colon cancer based on tumor deposits and extramural venous invasion on computed tomography. *JAMA Netw Open*. 2019;2(12):e1916987.
28. Lord AC, D'Souza N, Shaw A, et al. MRI-diagnosed tumor deposits and EMVI status have superior prognostic accuracy to current clinical TNM staging in rectal cancer. *Ann Surg*. 2022;276(2):334—344.
29. Hwang JH, Lim M, Han G, et al. Preparing pathological data to develop an artificial intelligence model in the nonclinical study. *Sci Rep*. 2023;13(1):3896.
30. Niazi MKK, Parwani AV, Gurcan MN. Digital pathology and artificial intelligence. *Lancet Oncol*. 2019;20(5):e253—e261.
31. Khan A, Brouwer N, Blank A, et al. Computer-assisted diagnosis of lymph node metastases in colorectal cancers using transfer learning with an ensemble model. *Mod Pathol*. 2023;36(5):100118.